Supplementary Material
Eco-evolutionary dynamics of decomposition: scaling up from microbial cooperation to ecosystem function

Elsa Abs[1,2*], Hélène Leman[3,4], and Régis Ferrière[2,5,6]

[1]*Department of Ecology and Evolutionary Biology, University of California, Irvine, CA 92697, USA.*
[2]*Interdisciplinary Center for Interdisciplinary Global Environmental Studies (iGLOBES), CNRS, Ecole Normale Supérieure, Paris Sciences & Lettres University, University of Arizona, Tucson AZ 85721, USA.*
[3]*Numed Inria team, UMPA UMR 5669, Ecole Normale Supérieure, 69364 Lyon, France.*
[4]*Centro de Investigación en Matemáticas, 36240 Guanajuato, México.*
[5]*Department of Ecology and Evolutionary Biology, University of Arizona, Tucson, AZ 85721, USA.*
[6]*Institut de Biologie (IBENS), Ecole Normale Supérieure, Paris Sciences & Lettres University, CNRS, INSERM, 75005 Paris, France.*

Elsa Abs: eabs@uci.edu: Corresponding author
Hélène Leman: helene.leman@inria.fr
Régis Ferrière: regisf@email.arizona.edu

Contents

1 Stochastic individual-based processes and rescaling

In the two following subsections are the proofs for steps 2 and 3 of the construction of the model in the first section of Methods in the main text of the article.

1.1 Reduction of the stochastic model from five to four state variables

The first model corresponds to the stochastic processes acting at the level of C, D, M, Z, X entities (molecules, cells) (Fig. 5a) within a microsite.

Dynamics of C, D, M, Z, X occur in continuous time. M_t is the number of bacterial cells at time t. Z_t, C_t, D_t are the numbers of enzyme molecules, SOC molecules, and DOC molecules, respectively. X_t is the number of complexes formed by an enzyme molecule binding a DOC molecule. DOC enters the microsite at a constant rate. When a cell dies, a fraction p of the molecules released are recycled into SOC, while the rest is recycled into DOC. A fraction l of dead microbes and deactivated enzymes may be lost due to leaching.

We denote by α the structural cost of a cell, which is the number of DOC molecules contained in one cell, and we denote by α' the energetic cost of a cell, which is the number of DOC molecules consumed to produce the energy needed for the synthesis reactions involved in the production of a cell. We denote the structural cost of one SOC molecule by β, and the structural and energetic cost of producing one molecule of enzyme by γ and γ', respectively. We assume that the energetic costs are carbon released by bacteria as CO_2 that diffuses out of the system instantaneously. We define the biomass production fraction and enzyme allocation fraction as

$$\bar{\gamma}_M := \frac{1}{\alpha + \alpha'}, \quad \bar{\gamma}_Z := \frac{1}{\gamma + \gamma'}. \tag{S.1}$$

The event times are given by independent exponential random variables whose parameters are defined by event rates (Tables S1 and S2). These event rates give an approximation of the average frequency of each event, however any event may occur at any time. The rates of cell growth and enzyme production depend on the cell trait φ. Cell division is the outcome of storing assimilated DOC until a threshold is reached. A parameter N scales the gradual process of consumption and storage of DOC. Thus, there can be growth only if there is enough D to cover both the structural cost, α/N, and the energetic cost, α'/N of this growth, hence the notation $\mathbf{1}_{\{D \geq (\alpha+\alpha')/N\}}$ which equals 1 if $D \geq (\alpha + \alpha')/N$, 0 otherwise. Likewise $\mathbf{1}_{\{D \geq \gamma+\gamma'\}}$ is used for the production event of an enzyme molecule. Growth leads to cell division only if enough D has been consumed and stored.

Enzyme-substrate complexes form at rate $\bar{\lambda}^K$ as one enzyme molecule (e.g. cellulase) bind one SOC molecule (e.g. cellulose). A complex may either dissociate (with no reaction) at rate $\bar{\lambda}^{\varepsilon}_{-1}$, or react at rate $\bar{\mu}^{\varepsilon}$ and convert the molecule of SOC into a molecule of DOC while the enzyme is released and free again to react with new molecules of SOC (Table S2).

We use K as a scaling parameter for the magnitude of the number of interacting bacteria, which by definition have access to the same (local) pool of resources. When $K = 1$, all parameter values

correspond to the rates observed for a volume of soil $V = 10^{-9}$ cm^3 that we take as the baseline volume expected to contain one cell. Increasing K means that the model treats interactions as well-mixed among an increasing number of cells that occupy an increasingly large volume. As a consequence, external inputs of SOC or DOC increase with K, and the probability that two enzyme and SOC molecules encounter, that is proportional to $\bar{\lambda}^K$, decreases. We thus assume that there are four constant parameters, $\bar{I}_C$, $\bar{I}_D$, $\bar{\lambda}$ and $\bar{K}_{mU}$, such that

$$\bar{I}_C^K = K\bar{I}_C,\ \bar{I}_D^K = K\bar{I}_D,\ \bar{\lambda}^K = \frac{\lambda}{K} \text{ and } \bar{K}_{mU}^K = K\bar{K}_{mU} \tag{S.2}$$

where $\bar{I}_C$ is the external input of C, $\bar{I}_D$ is the external input of D, $\bar{\lambda}$ is the encountering rate, and $\bar{K}_{mU}$ is the uptake half-saturation constant. In our simulations, we will generally assume that K is equal to 10, which is a good approximation of the number of cells that interact at each time.

Let K be fixed and let

$$C^\varepsilon(t), D^\varepsilon(t), M^\varepsilon(t), Z^\varepsilon(t), X^\varepsilon(t)$$

designate the (stochastic) number of cells, enzymes molecules, SOC molecules, complexes and DOC molecules at time t in the CDMZX model associated to parameters $\bar{\lambda}_{-1}^\varepsilon$ and $\bar{\mu}^\varepsilon$. Next theorem ensures that under the assumption that complex dissociation and the decomposition reaction of the complex are much faster than complex formation:

$$\bar{\lambda}_{-1}^\varepsilon,\ \bar{\mu}^\varepsilon >> \bar{\lambda}^K,$$

the stochastic CDMZX model can be simplified into the four-compartment stochastic CDMZ model with structure shown in Fig. 5b and events and event rates listed in Table S2 with

$$\bar{V}_{mD}^K = \bar{\lambda}^K \frac{\bar{\mu}}{\bar{\mu} + \bar{\lambda}_{-1}} := \frac{\bar{V}_{mD}}{K}, \tag{S.3}$$

where $\bar{V}_{mD}$ corresponds to the maximum decomposition rate when C is not limiting.

Precisely, we assume that there are two positive constant $\bar{\lambda}_{-1}$ and $\bar{\mu}$ such that

$$\bar{\lambda}_{-1}^\varepsilon = \frac{1}{\varepsilon}\bar{\lambda}_{-1} \quad \text{and} \quad \bar{\mu}^\varepsilon = \frac{1}{\varepsilon}\bar{\mu}. \tag{S.4}$$

Let

$$\mathbb{Y}^\varepsilon := (M^\varepsilon, Z^\varepsilon + X^\varepsilon, C^\varepsilon + X^\varepsilon, D^\varepsilon),$$

then the following result, which is proved in Section 4, holds.

Theorem 1. *Assume that* (S.4) *holds and that* $(M^\varepsilon, Z^\varepsilon, C^\varepsilon, X^\varepsilon, D^\varepsilon)(0)$ *converges in* L^2 *to the deterministic vector* $(M_0, Z_0, C_0, 0, D_0)$*, when* ε *goes to* 0*, then for any* $T \geq 0$*, the sequence of processes* $(\mathbb{Y}^\varepsilon(t), t \in [0,T])_{\varepsilon>0}$ *converges in law, in* $\mathbb{D}([0,T], \mathbb{N}^4)$ *endowed with the Skorohod topology, to* $(M, Z, C, D)_{t\in[0,T]}$ *defined by the 4-boxes model whose rates are described in Table S2, initial condition is* (M_0, Z_0, C_0, D_0) *and* $\bar{V}_{mD}^K$ *is defined by* (S.3)*.*

Table S1. Events involving enzyme-SOC complexes (X) in the CDMZX model. Individual-level events and event rates.

Event	Event rate
Formation of 1 complex X from 1 Z and 1 C: $(M, Z, C, X, D) \mapsto (M, Z-1, C-1, X+1, D)$	$\bar{\lambda}^K ZC$
Dissociation of 1 complex X into 1 Z and 1 C: $(M, Z, C, X, D) \mapsto (M, Z+1, C+1, X-1, D)$	$\bar{\lambda}^{\varepsilon}_{-1} X$
Depolymerization of 1 C into β D (decomposition) from the effect of Z on C in complex X $(M, Z, C, X, D) \mapsto (M, Z+1, C, X-1, D+\beta)$	$\bar{\mu}^{\varepsilon} X$

Table S2. Events and event rates in both stochastic models (CDMZ and CDMZX). Cells are characterized by their trait value φ.

Event	Event rate
Events relative to M	
M grows and accumulates an equivalent of α/N molecules of DOC, gives birth to an offspring if its stock of carbon is equal to α $D \mapsto D - \frac{\alpha+\alpha'}{N}$	$N(1-\varphi)\bar{\gamma}_M \bar{V}_{mU} \frac{D}{\bar{K}^K_{mU}+D} \mathbf{1}_{\left\{D \geq \frac{\alpha+\alpha'}{N}\right\}}$
M dies $C \mapsto C + \lfloor (1-l) p \frac{\alpha}{\beta} \rfloor$, $D \mapsto D + \lfloor (1-l)(1-p)\alpha \rfloor$	$\bar{d}_M$
M produces 1 Z $D \mapsto D - (\gamma + \gamma')$	$\varphi \bar{\gamma}_Z \bar{V}_{mU} \frac{D}{\bar{K}^K_{mU}+D} \mathbf{1}_{\{D \geq \gamma+\gamma'\}}$
Events specific to Z, C, D	
Deactivation of 1 Z: $(M, Z, C, D) \mapsto (M, Z-1, C, D + \lfloor (1-l)\gamma \rfloor)$	$\bar{d}_Z Z$
External input of 1 C: $(M, Z, C, D) \mapsto (M, Z, C+1, D)$	$\bar{I}^K_C$
Loss of 1 C due to leaching: $(M, Z, C, D) \mapsto (M, Z, C-1, D)$	$\bar{e}_C C$
External input of 1 D: $(M, Z, C, D) \mapsto (M, Z, C, D+1)$	$\bar{I}^K_D$
Loss of 1 D due to leaching:	

$(M, Z, C, D) \mapsto (M, Z, C, D-1)$	$\bar{e}_D D$
Event specific to CDMZ model	
Depolymerization of 1 C into β D (decomposition) through enzymatic reaction $(M, Z, C, D) \mapsto (M, Z+1, C-1, D+\beta)$	$\bar{V}^K_{mD} ZC$

1.2 Derivation of the hybrid stochastic-deterministic model by rescaling the stochastic CDMZ model

As explained in Methods in the main text, the biomass represented by a cell is much larger than the carbon mass of a molecule of enzyme, SOC or DOC, whereas the number of cells is much smaller than the number of enzyme, SOC and DOC molecules. We took this into account for approximating the stochastic CDMZ individual-based model by a hybrid deterministic-stochastic model, which allows to accelerate consequently the model simulations.

To set the approximation rigorously, we introduce a parameter κ that gives the order of magnitude of the biomass of a cell and the number of enzymes, SOC and DOC molecules.

The structural and energetic costs of a bacteria is rewritten

$$\alpha_\kappa := \kappa\alpha \quad \text{and} \quad \alpha'_\kappa = \kappa\alpha'.$$

We also set $\bar{I}^\kappa_C = \kappa \bar{I}_C$, $\bar{I}^\kappa_D = \kappa \bar{I}_D$, $\bar{V}^\kappa_{mD} = \frac{\bar{V}_{mD}}{\kappa}$, $\bar{K}^\kappa_{mU} = \kappa \bar{K}_{mU}$, and we are interested in the sequence

$$\left(M^\kappa_t, \omega_Z \frac{Z^\kappa_t}{\kappa}, \omega_C \frac{C^\kappa_t}{\kappa}, \omega_D \frac{D^\kappa_t}{\kappa}, t \geq 0 \right)_{\kappa \geq 0},$$

when κ converges to ∞. ω_Z is the averaged carbon mass content of one enzyme, and likewise for cells (ω_M), SOC (ω_C) and DOC (ω_D). The ω parameters are related to α, β and γ according to:

$$\alpha = \frac{\omega_M}{\omega_D}, \quad \beta = \frac{\omega_C}{\omega_D}, \quad \text{and} \quad \gamma = \frac{\omega_Z}{\omega_D}. \tag{S.5}$$

Using these rescaling parameters allows the system of equations to be expressed in biomass and not in molecular density, which would be less meaningful and more difficult to interpret.

With further rescaling (such that all parameters of the system are expressed in biomass) and notations:

$$\begin{array}{lllllllll}
I_C & := & \omega_C \bar{I}_C, & I_D & := & \omega_D \bar{I}_D, & K_{mU} & := & \omega_D \bar{K}_{mU}, \\
V_{mD} & := & \frac{1}{\omega_Z} \bar{V}_{mD}, & V_{mU} & := & \frac{\omega_D}{\omega_M} \bar{V}_{mU}, & \gamma_M & := & \frac{\omega_M}{\omega_D} \bar{\gamma}_M, \qquad \gamma_Z := \frac{\omega_Z}{\omega_D} \bar{\gamma}_Z, \\
d_M & := & \bar{d}_M, & d_Z & := & \bar{d}_Z, & e_C & := & \bar{e}_C, \qquad e_D := \bar{e}_D,
\end{array} \tag{S.6}$$

a direct application of Theorem 3.1 of Crudu et al. [2012] gives the following theorem.

Theorem 2. *Assume that* $\left(M^\kappa(0), \omega_Z \frac{Z^\kappa(0)}{\kappa}, \omega_C \frac{C^\kappa(0)}{\kappa}, \omega_D \frac{D^\kappa(0)}{\kappa}\right)$ *converges to a deterministic vector* (M_0, z_0, c_0, d_0)*, then the sequence of processes*

$$\left(M_t^\kappa, \omega_Z \frac{Z_t^\kappa}{\kappa}, \omega_C \frac{C_t^\kappa}{\kappa}, \omega_D \frac{D_t^\kappa}{\kappa}, t \geq 0\right)$$

converges in distribution, when κ *goes to* $+\infty$*, to the distribution of a PDMP whose generator is*

$$\begin{aligned}
&\mathcal{A}f(M,z,c,d) = \\
&\quad (1-\varphi)\gamma_M V_{mU} \frac{d}{K_{mU}+d} M \mathbf{1}_{\{d \geq \omega_D(\alpha+\alpha')\}} \Big[f\left(M+1, z, c, d-\omega_D(\alpha+\alpha')\right) - f(M,z,c,d) \Big] \\
&\quad + \bar{d}_M M \Big[f\left(M-1, z, c+(1-\varepsilon)p\alpha\omega_D, d+(1-\varepsilon)(1-p)\alpha\omega_D\right) - f(M,z,c,d) \Big] \\
&\quad + \left(\varphi\eta\omega_D V_{mU}\gamma_Z \frac{d}{K_{mU}+d} M - d_Z z \right) \frac{\partial f(M,z,c,d)}{\partial z} \\
&\quad + \left(I_C - l_C c - V_{mD} z c\right) \frac{\partial f(M,z,c,d)}{\partial c} \\
&\quad + \left(I_D - l_D d + V_{mD} z c + (1-\varepsilon) d_Z z - \varphi\eta V_{mU} \frac{d}{K_{mU}+d} M \right) \frac{\partial f(M,z,c,d)}{\partial d}.
\end{aligned}$$

This generator corresponds precisely to the generator of the PDMP described at the end of Section 2.1 of the article.

For the sake of simplicity, the theorem has been written in the case where $N = 1$ in the CDMZ model, however, it can be directly adapted for $N > 1$. In our context, approximating the microscopic model by the limiting PDMP is justified due to the large values of $\alpha_\kappa = 10^{10}$ and $\alpha'_\kappa = 2.33 \cdot 10^{10}$ compared to β, γ and γ' (less than 10^4). Finally, when N is really large, we consider that the growth of all cells is also deterministic. However, a rigorous proof of this approximation is not given in this paper.

2 Simulation algorithm

In this section, we describe the algorithm used to simulate our final model, which is a hybrid stochastic-deterministic model on the lattice, and used to perform the figures of the paper. The algorithm is adapted from the ones presented for example in Champagnat et al. [2006], Fournier and Méléard [2004], also known as Gillepsie algorithm [Kierzek, 2002] and from the ones to simulate PDMP.

The main idea is to couple PDMP models locally among microsites, by accounting for the diffusion of products (DOC) and dispersal of cells between adjacent microsites. The DOC diffusion between microsites is modelled by approximating a continuous diffusion with a Euler scheme in which time is discretized with a fixed time step interval, τ_{diff}. τ_{diff} is chosen sufficiently small to have a good discretization of the DOC diffusion.

Precisely, the simulation starts with a given amount of M, z, c and d in each microsite at time $t = 0$. Two stochastic events (death of a bacteria) can never occur at the same time. Assume that the process has been computed until time t_i and let us explain how to compute it until time t_{i+1}.

We first simulate T, an exponential random variable with parameter $r(t_i) = \bar{d}_M M(t_i)$, which corresponds to the death rate of the total bacteria population at time t_i ($M(t_i)$ being the total number of bacteria on the entire lattice). And we compute

$$t_{i+1} := t_i + \min\left(T, \tau_{\text{diff}}\right).$$

In order to obtain the quantities of enzymes, SOC and DOC (resp. $z(t_{i+1})$, $c(t_{i+1})$, and $d(t_{i+1})$) in biomass in each microsite at time t_{i+1} and the variation in amount of DOC stored within a bacteria in the corresponding microsite, we use an Euler scheme that solves the dynamical system

$$\begin{cases} z'(t) = \varphi\alpha\omega_D V_{mU}\gamma_Z \dfrac{d}{K_{mU}+d} M - d_Z z \\ c'(t) = I_C - l_C c - V_{mD} z c \\ d'(t) = I_D - l_D d + V_{mD} z c + (1-l) d_Z z - \varphi\alpha V_{mU} \dfrac{d}{K_{mU}+d} M \\ \Delta'(t) = \alpha(1-\varphi)\gamma_M V_{mU} \dfrac{d}{K_{mU}+d}, \end{cases}$$

in each microsite between t_i and t_{i+1}, where M is the number of bacteria in the microsite at time t_i, Δ gives the amount variation of DOC stored within a bacteria, $\Delta(t_i) = 0$ and the other initial conditions are the biomass of z, c, d in the corresponding microsite at time t_i.

Note that, within a microsite, the amount variation of stored DOC is equal for all bacteria and corresponds to $\Delta(t_{i+1})$. Hence, this amount is added to the amount of DOC stored within each bacteria living in the corresponding microsite. If, for a bacteria k, the resulting amount $\tilde{S}_k(t_{i+1})$ is over α, a new bacteria appears. The amount of stored DOC within the new cell and the mother cell is then updated to be equal to half of $\tilde{S}_k(t_{i+1}) - \alpha$. To determine the position of the new bacteria, the following steps are followed:

- A uniform random variable θ_1 in $[0, 1]$ is thrown.
- If $\theta_1 < 1 - p_{disp}$, the new bacteria is added to the mother cell microsite.
- Otherwise, the new bacteria disperses:
  - If empty microsites are available in the four nearest microsites, the new cell is added to one of them, drawn randomly.
  - Otherwise, a uniform random variable θ_2 in $[0, 1]$ is thrown:
    - If $\theta_2 < 1 - p_{open}$, the new cell is added in the mother cell microsite.
    - If $\theta_2 \geq 1 - p_{open}$, a micro-disturbance happens. That is, one of the four nearest microsites is chosen at random. All bacteria in this microsite dies. These cells are removed from the population, an amount of $(1-\varepsilon)p\omega_D\alpha M$ is added to variable d and an amount of $(1-\varepsilon)(1-p)\omega_D\alpha M$ is added to variable c in this microsite (where M is the number of dead cells). Finally, the new bacteria is placed in this microsite.

Our next step in the algorithm consists in imitating a step of the Euler scheme associated with the diffusion equation

$$\frac{d}{dt}d(x,t) = \sigma_{\text{diff}}\Delta d(x,t),$$

in order to mimicking the diffusion of DOC. To this aim, we update the DOC biomass $d_{j,l}(t_{i+1})$ in the microsite of the j^{th} column and the l^{th} line by replacing it with

$$d_{j,l}(t_{i+1}) + \frac{\sigma_{\text{diff}} \cdot \tau}{(VK)^{2/3}}\Big(d_{j+1,l}(t_{i+1}) + d_{j-1,l}(t_{i+1}) + d_{j,l+1}(t_{i+1}) + d_{j,l-1}(t_{i+1}) - 4 * d_{j,l}(t_{i+1})\Big).$$

Once these previous steps of updating are computed, we verify if a bacteria actually dies at time t_{i+1}.

- If $t_{i+1} - t_i = T$, then a bacteria dies at time t_{i+1}. It is chosen uniformly at random among all alive cells and it is removed from the population. At the same time, an amount of $(1-\varepsilon)p\omega_D\alpha$ is added to variable d and an amount of $(1-\varepsilon)(1-p)\omega_D\alpha$ is added to variable c in the corresponding microsite.
- If $t_{i+1} - t_i = \tau_{\text{diff}}$ (i.e. $T > \tau_{\text{diff}}$), no bacteria dies.

All steps are then computed again until a chosen time is reached or until all cells are dead.

3 Parameter values and numerical simulations

In order to evaluate the parameters of our model and give default values based on literature, we compare the stochastic CDMZ individual-based model (which is our default model) to a deterministic one. Under the assumption that all entities are in large number, the CDMZ model can be rescaled as a dynamical system of ordinary differential equations, similar to Schimel and Weintraub [2003] seminal model of litter decomposition (see also Abs and Ferrière [2020], Wieder et al. [2015]). We obtain the scaling of the deterministic model parameters relative to the individual-level process parameters.

3.1 Deterministic approximation of the stochastic CDMZ model

In this subsection we assume that all cells have the same trait value, φ, so that there is only one type of cells in the system, and we will consider that K is large, where K refers to the scaling parameter introduce in Section 1.1. If (S.2) holds, we prove that the stochastic CDMZ model can be approximated by the following deterministic model

$$\begin{cases} \dfrac{dm}{dt} = (1-\varphi)\gamma_M V_{mU}\dfrac{d}{K_{mU}+d}m - d_M m \\ \dfrac{dz}{dt} = \varphi\gamma_Z V_{mU}\dfrac{d}{K_{mU}+d}m - d_Z z \\ \dfrac{dc}{dt} = I_C - e_C c + (1-l)pd_M m - V_{mD}zc \\ \dfrac{dd}{dt} = I_D - e_D d + V_{mD}zc + (1-l)\left[(1-p)d_M m + d_Z z\right] - V_{mU}\dfrac{d}{K_{mU}+d}m, \end{cases} \tag{S.7}$$

where m, z, c and d are in carbon mass unit, and all parameters correspond to rescaled parameters defined in (S.6).

Precisely, let us denote by $(M^K(t), Z^K(t), C^K(t), D^K(t))$ the number of bacteria, enzymes molecules, SOC molecules and DOC molecules given by the stochastic CDMZ model presented in Section 1.1 in the case of K neighborhoods. The following lemma can be deduced from a direct application of Chapter 11 in Ethier and Kurtz [2009].

Lemma 3.1. *Assume that* (S.2) *holds and that*

$$\left(\omega_M \frac{M^K(0)}{K}, \omega_Z \frac{Z^K(0)}{K}, \omega_C \frac{C^K(0)}{K}, \omega_D \frac{D^K(0)}{K}\right) \underset{K\to+\infty}{\longrightarrow} (m(0), z(0), c(0), d(0)) \in [0, +\infty)^4,$$

then for any $T \geq 0$,

$$\lim_{K\to+\infty} \sup_{t\leq T} \left\| \left(\omega_M \frac{M^K(t)}{K}, \omega_Z \frac{Z^K(t)}{K}, \omega_C \frac{C^K(t)}{K}, \omega_D \frac{D^K(t)}{K}\right) - (m(t), z(t), c(t), d(t)) \right\|_\infty = 0,$$

where the limit stands in probability, $\|.\|_\infty$ *denotes the* L^∞*-norm on* $\mathbb{R}^4$ *and* (m, z, c, d) *is the unique solution to* (S.7) *with initial condition* $(m(0), z(0), c(0), d(0))$.

3.2 Default parameter values and initialization of simulations

Model (S.7) can be compared to models already existing in the literature, which provide us with default parameter values (Allison et al. [2010], German et al. [2012], Hagerty et al. [2014], Schimel and Weintraub [2003]).

The structural and energetic costs (αs and γs) are calculated from the masses and production fractions of the variables (see Equations (S.1) and (S.5)). They are not inputs of the model, and are presented here only for informative purposes.

Table S3. Parameters of the deterministic model in biomass.

Parameter	Unit	Description	Default value
V	cm^3	microsite volume	10^{-9}
K		scaling parameter of (local) microbial population size	10
φ		enzyme allocation fraction	$[0, 1]$
γ_M		microbial carbon biomass production fraction	0.3
γ_Z		enzyme carbon mass production fraction	0.4
ω_M	mg	mass of 1 M cell	10^{-9}
ω_Z	mg	mass of 1 Z molecule	10^{-16}
ω_C	mg	mass of 1 C molecule	10^{-16}
ω_D	mg	mass of 1 D molecule	10^{-19}
α		structural cost in D of 1 M cell	10^{10}
α'		energetic cost in D of 1 M cell	2.33×10^{10}

β		structural cost in D of 1 C molecule	10^3
γ		structural cost in D of 1 Z molecule	10^3
γ'		energetic cost in D of 1 Z molecule	1.5×10^3
d_M	h^{-1}	microbial carbon biomass death rate	2×10^{-4}
d_Z	h^{-1}	enzyme carbon mass deactivation rate	2×10^{-3}
V_{mU}	h^{-1}	maximum uptake rate (in carbon mass)	0.42
V_{mD}	$mg^{-1}h^{-1}$	maximum decomposition rate when C is not limiting	$\frac{7\times10^{-4}}{V}$
K_{mU}	mg	uptake half-saturation constant	$0.3 \times V$
I_C	mgh^{-1}	external input of C	$5 \times 10^{-4} \times V$
I_D	mgh^{-1}	external input of D	0
e_C	h^{-1}	C leaching rate	10^{-6}
e_D	h^{-1}	D leaching rate	10^{-6}
l		fraction of dead M and deactivated Z leached instead of recycled	0
p		fraction of recycled dead M flowing into C (remaining fraction flows into D)	0.5
$T_{\max}$	h	maximum simulation time	10^6
p_{mut}		probability of mutation per cell division event	between $1/(Kln(K))$ and $1/K^2$
σ_{mut}		standard deviation of mutation effect	$[0.01 - 0.1]$

The decomposition rate V_{mD} has been calculated as $\frac{v^D_{max}}{K^D_m}$ from Allison et al. [2010]'s model. Since the stochastic model allows us to look at the behaviour of smaller populations, we reduce the soil volume to $10^{-9}cm^3$ (instead of $1cm^3$ in most models). Volume affects 3 parameters: V_{mD}, K_{mU}, and I_C. We ignore the input of D. We assumed leaching of D equal to leaching of C. Dead microbes and deactivated enzymes are recycled half into C and the other half into D. The values for p_{mut} and σ_{mut} have been chosen to respect the assumptions of the adaptive dynamics that mutations are rare and small [Geritz et al., 1998].

Concerning the change of unit from biomass to individuals (ωs), the models for M, Z, C, D are *Bacillus subtilis* ou *clausii*, cellulase, cellulose and glucose respectively. We estimated the mass of 1 D with the mass of 1 molecule of glucose, which contains 6 atoms of carbon and $m_{6.02\times10^{23}atoms\ of\ ^{12}C} = 12g$. We estimated the mass of 1 C from the approximation that 1 molecule of cellulose contains about 10^3 molecules of glucose. We estimated the mass of 1 Z by assuming that 1 molecule of cellulase contains about as much carbon as 1 molecule of cellulose. Finally, we estimated the mass of 1 M based on the results from biomass estimations of soil samples (with various methods: CFI, CFE, SIR...) that there are about 4×10^8 active individual bacteria in $1cm^3$ of bulk soil, which weight $0.1mg$ in carbon [Fierer et al., 2009].

Finally, microsites are initialized according to the stationary state given by System (S.7) for all variables M, Z, C and D. Mutants are initially located at the center of the grid (changing the initial location does not modify the final fraction of mutants in the grid). To reduce simulation time, we assume that mutants are initially at 5% frequency in the introduction microsite. We ran simulations for (resident, mutant) pairs with +/- 0.05 difference in trait value φ . From the final frequency of mutants we compute the mutant exponential growth rate, and average over 20 simulation replicates.

3.3 Numerical comparison of the hybrid stochastic-deterministic model and its deterministic approximation

The deterministic model corresponds to a large (high K) single-microsite version of the final hybrid stochastic-deterministic model used for our results. Its ecological dynamics defined in (S.7) can be analytically solved, indicating that there are one or three equilibria depending on the value of φ. At the "trivial" equilibrium, there are no active microbes or enzymes ($M_{eq1} = Z_{eq1} = 0$), SOC and DOC are fixed by the balance of external inputs and leaching ($C_{eq1} = I_C/e_C$ and $D_{eq1} = I_D/e_D$). This equilibrium is always locally stable. When the other two equilibria exist, one is always unstable, and M, Z, C, D at both equilibria are all positive. Existence of the positive equilibria depends on φ belonging to a certain interval ($\varphi_{min} \leq \varphi \leq \varphi_{max}$). When the non-trivial equilibria exist, one is unstable and the other is locally stable for most values of φ and unstable (bifurcating into a limit cycle) for values of φ close to φ_{min}. For the default parameters values (Table S3), both exist when $0.01212 < \varphi < 0.9984$ and the microbial equilibrium is stable for $0.01212 < \varphi < 0.9969$.

For viable values of φ (between 0.01212 and 0.9969), microbes do not go extinct during the simulated time in both the single-microsite hybrid model with large K and the deterministic model despite possible strong oscillations around the equilibrium. However as we decrease the system size K, the average microbial population size M decreases in the hybrid model, and stochasticity added to fluctuations can lead to rapid extinction, resulting in a smaller range of viable φ (Fig. S1). We can find a minimal value of K under which the range of viable φ diverges significantly from deterministic predictions. We can lower this minimal value when switching to a multi-microsites grid (Fig. S2), because local extinctions do not occur simultaneously, therefore the population at the grid scale can survive one microsite population extinction, and dead cells are recycled into resource, which feed and help survival of neighbouring microsites' populations.

How well does the deterministic CDMZ model capture the behavior of its stochastic counterpart? A key difference comes from the fact that a cell can grow only if there is enough D available for both the structural and the energetic costs of growth, $(\alpha + \alpha')/N$, and likewise for the production of enzyme molecules. If there is not enough D, the event is dropped, which means that the cell does not grow and no D is consumed, therefore the numbers of M, Z and D are unchanged. This does not happen in the deterministic model, which is a infinite population approximation of the stochastic model. In particular, since one cell is much more costly in D than one enzyme

molecule (Table S3), more events of cell division than enzyme production may be dropped, especially when N is small. As a result, a significant difference may arise between the expected investment (parameter φ) and realized investment of a cell into enzyme production versus biomass production. Figure S1 shows that at low system size K, keeping the discrepancy small between the deterministic and stochastic models across the range of feasible φ, requires outstandingly large N, so that the structural and energetic costs of growth are kept very low.

A second key difference is fluctuations in the stochastic model, which may drive the population to extinction. In contrast, for viable values of φ, strong oscillations may occur in the deterministic model without compromising the cell population persistence. In the stochastic, spatially extended system, the habitat spatial structure induces a metapopulation rescue effect, which strongly increases the probability of persistence over any given time horizon (Fig. S2).

3.4 Resident-mutant interaction in the spatial model

At each birth event, a daughter cell is a mutant with probability p_{mut}, or has the same φ value that its mother with probability $(1 - p_{mut})$. Because only one event can occur in any small time interval, only one mutant can appear in any small time step but multiple mutants with different φ values can co-occur. We aim to look at (1) the dynamics of the trait φ, (2) the fate of the population with vs. without adaptive evolution (fixed $p_{mut} = 0$).

We initialize the simulation with a monomorphic population (all cells have the same φ value). All 4 variables c, d, z, M are initialized at the steady state values predicted by the deterministic model corresponding to the values of K and φ chosen. We run 20 simulations per test (e.g. for each K tested, for each initial φ tested, for with versus without evolution), which are different due to demographic stochasticity. Total time of all parallelized simulations was 10^7 hours (about 1000 years).

4 Rigorous proof of Theorem 1

In this Section, we prove rigorously Theorem 1. To reduce the CDMZX model, the main difficulty arises because we can not have classical Skorohod convergence in distribution of the process $(M^\varepsilon, Z^\varepsilon, C^\varepsilon, X^\varepsilon, D^\varepsilon, t \in [0,T])_{\varepsilon>0}$. Indeed, when ε is small, there will be some really close jumps of X^ε when a complex is formed and almost immediately dissociated or decomposed. It is why we are interested in the process

$$\mathbb{Y}^\varepsilon := (M^\varepsilon, Z^\varepsilon + X^\varepsilon, C^\varepsilon + X^\varepsilon, D^\varepsilon),$$

and we prove the convergence of the sequence of processes $(\mathbb{Y}^\varepsilon(t), t \in [0,T])_{\varepsilon>0}$ in law, in $\mathbb{D}([0,T], \mathbb{N}^4)$ endowed with the Skorohod topology, to $(M, Z, C, D)_{t\in[0,T]}$ defined by the 4-boxes model of Section 1.1.

Here we take $N = 1$, but the proof could be generalized $N > 1$ by introducing multiple cell stages describing the state of cell resource reserve.

Proof. **Step 1**: The first step is to prove the tightness of sequence $(\mathbb{Y}^\varepsilon)_{\varepsilon>0}$ in $\mathbb{D}([0,T],\mathbb{N}^4)$. To this aim, we denote the jumps set of process $(\mathbb{Y}^\varepsilon(t), t\in[0,T])$ by

$$\{J_j^\varepsilon\}_{j\geq 1} = \{t\in[0,T], \mathbb{Y}^\varepsilon(t-) \neq \mathbb{Y}^\varepsilon(t)\}. \tag{S.8}$$

Note that $\mathbb{Y}^\varepsilon$ is càdlàg, hence the definition (S.8). As any jump of $\mathbb{Y}^\varepsilon$ is of size 1, the tightness of $\mathbb{Y}^\varepsilon$ follows from the two conditions:

i) $\lim_{a\to+\infty} \limsup_{\varepsilon\to 0} \mathbb{P}(\|\mathbb{Y}^\varepsilon\|_\infty \geq a) = 0$,

ii) $\lim_{\delta\to 0} \limsup_{\varepsilon\to 0} \mathbb{P}(\exists j\geq 0, J_{j+1}^\varepsilon - J_j^\varepsilon \leq \delta) = 0$.

Indeed, these two conditions directly imply the two conditions of Theorem 13.2 in the book of Billingsley [2013], which ensures tightness.

To prove i), we introduce $N_{Tot}^\varepsilon = \alpha M^\varepsilon + \gamma Z^\varepsilon + \beta C^\varepsilon + (\gamma+\beta)X^\varepsilon + D^\varepsilon$ the total equivalent number of DOC molecules in the system at any time. Since the only external sources of carbon are inputs of C and D, N_{Tot}^ε is stochastically bounded from above by

$$\sup_{s\leq T} N_{Tot}^\varepsilon(s) \preceq N_{Tot}^\varepsilon(0) + \mathcal{P}((\bar{I}_D + \beta\bar{I}_C)T) =: N_{\max}^\varepsilon, \tag{S.9}$$

where $\mathcal{P}((\bar{I}_D + \beta\bar{I}_C)T)$ is a Poisson random variable with parameter $(\bar{I}_D + \beta\bar{I}_C)T$. From the assumption on the initial conditions, we deduce immediately that the random variable $N_{\max}^\varepsilon$ is L^2-integrable and that for ε sufficiently small, there exists $C_0 > 0$ such that

$$\mathbb{E}\left[N_{\max}^\varepsilon\right] + \mathbb{E}\left[(N_{\max}^\varepsilon)^2\right] \leq C_0. \tag{S.10}$$

Moreover, since α, β and γ are greater than 1, we obtain from Markov inequality,

$$\mathbb{P}(\|\mathbb{Y}^\varepsilon\|_\infty \geq a) \leq \mathbb{P}(N_{\max}^\varepsilon \geq a) \leq \frac{1}{a} C_0,$$

for any ε sufficiently small. This ends the proof of i).

We now deal with ii). Let us set $\eta > 0$. First of all, note that we can focus the study on the set $\{X^\varepsilon(0) = 0\}$. Indeed, from the assumption on the initial condition, for any ε small enough, $\mathbb{P}(X^\varepsilon(0) \geq 1) \leq \eta$. Hence

$$\mathbb{P}(\exists j\geq 0, J_{j+1}^\varepsilon - J_j^\varepsilon \leq \delta) \;\leq\; \eta + \mathbb{P}_0(\exists j\geq 0, J_{j+1}^\varepsilon - J_j^\varepsilon \leq \delta), \tag{S.11}$$

where for any set $\mathcal{A}$, $\mathbb{P}_0(\mathcal{A}) = \mathbb{P}(\mathcal{A}|X^\varepsilon(0)=0)$. In what follows, we restrict our focus on $\{X^\varepsilon(0)=0\}$.

Then, we count the number of jumps of $\mathbb{Y}^\varepsilon$. Note that any jump of $\mathbb{Y}^\varepsilon$ is also a jump of $(M^\varepsilon, Z^\varepsilon, C^\varepsilon, X^\varepsilon, D^\varepsilon)$. Thus, we count the jumps number of the latter. As originally done by Fournier and Méléard [2004], it is convenient to represent a trajectory of individual-based processes as the unique solution of a system of stochastic differential equations driven by Poisson point measures. To this aim, we introduce a collection of 11 independent Poisson Point Processes

$(N^i(\mathrm{d}s,\mathrm{d}\theta))_{i=1,..,11}$ on $[0,\infty)^2$ with intensity $\mathrm{d}s\mathrm{d}\theta$ and independent of ε, which will be used to encode the 11 different types of events of the process $(M^\varepsilon, Z^\varepsilon, C^\varepsilon, X^\varepsilon, D^\varepsilon)$. We also denote all rates of this process by $(r_i^\varepsilon(t), t\in[0,T])_{i=1,..,11}$, i.e. these rates are respectively $(1-\varphi)\bar\gamma_M \bar V_{mU}\frac{D^\varepsilon}{K_{mU}+D^\varepsilon}M^\varepsilon \mathbf{1}_{\{D^\varepsilon\geq\alpha+\alpha'\}}$ (birth of a M), $\bar d_M M^\varepsilon$ (death of a M), $\varphi\bar\gamma_Z\bar V_{mU}\frac{D^\varepsilon}{K_{mU}+D^\varepsilon}M^\varepsilon\mathbf{1}_{\{D^\varepsilon\geq\gamma+\gamma'\}}$ (production of a Z), $\bar d_Z Z^\varepsilon$ (deactivation of a Z), $\bar I_C$ (appearance of a C), $\bar e_C C^\varepsilon$ (disappearance of a C), $\bar I_D$ (appearance of a D), $\bar e_D D^\varepsilon$ (disappearance of a D), $\bar\lambda Z^\varepsilon C^\varepsilon$ (formation of a X), $\bar\lambda^\varepsilon_{-1}X^\varepsilon$ (dissociation of a X), and $\bar\mu^\varepsilon X^\varepsilon$ (decomposition of a X). Note that only the events of type 1 to 8 and 11 correspond to jumps of $\mathbb{Y}^\varepsilon$. Hence, the jumps number of $\mathbb{Y}^\varepsilon$ can be bounded stochastically by

$$\sharp\{J_j^\varepsilon\} \preceq \sum_{i\in\{1,..,8,11\}}\int_0^T\int_{\mathbb{R}^+}\mathbf{1}_{\{\theta\leq r_i^\varepsilon(s-)\}}N^i(\mathrm{d}s,\mathrm{d}\theta). \tag{S.12}$$

The only problem comes from the last rate $\bar\mu^\varepsilon X^\varepsilon$, which is unbounded when ε goes to 0. However $\bar\mu^\varepsilon X^\varepsilon = 0$ as soon as there is no complex X in the system, and complexes are created with the encounter of a Z and a C (9-th rate). Thus, we immediately conclude that

$$\int_0^T\int_{\mathbb{R}^+}\mathbf{1}_{\{\theta\leq\bar\mu^\varepsilon X^\varepsilon(s-)\}}N^{11}(\mathrm{d}s,\mathrm{d}\theta)\leq\int_0^T\int_{\mathbb{R}^+}\mathbf{1}_{\{\theta\leq\bar\lambda Z^\varepsilon(s-)C^\varepsilon(s-)\}}N^9(\mathrm{d}s,\mathrm{d}\theta).$$

In addition with (S.12), (S.9) and (S.10), we deduce, if ε is small enough that

$$\begin{aligned}\mathbb{P}_0(\sharp\{J_j^\varepsilon\}>n) &\leq \sum_{i=1}^9\mathbb{P}_0\left(\int_0^T\int_{\mathbb{R}^+}\mathbf{1}_{\{\theta\leq r_i^\varepsilon(s-)\}}N^i(\mathrm{d}s,\mathrm{d}\theta)\geq\frac{n}{9}\right)\\ &\leq \frac{9}{n}T\sum_{i=1}^9\mathbb{E}_0\left[\sup_{s\in[0,T]}r_i^\varepsilon(s)\right]\\ &\leq \frac{9T}{n}\Big(\bar I_C+\bar I_D+C_1\mathbb{E}_0\left[N^\varepsilon_{\max}\right]+\bar\lambda\mathbb{E}_0\left[(N^\varepsilon_{\max})^2\right]\Big)\\ &\leq \frac{9T}{n}C_2\underset{n\to+\infty}{\longrightarrow}0,\end{aligned} \tag{S.13}$$

with $C_1 := \bar\gamma_M\bar V_{mU}+\bar d_M+\bar\gamma_Z\bar V_{mU}+\bar d_Z+\bar e_C+\bar e_D$ and $C_2 := \bar I_C+\bar I_D+C_1C_0+\bar\lambda C_0$. We fix $n := \lfloor 9TC_2/\eta\rfloor+1$ such that the last r.h.s. is smaller than η. Thus,

$$\begin{aligned}\mathbb{P}_0(\exists j\geq0, J_{j+1}^\varepsilon-J_j^\varepsilon\leq\delta) &\leq \mathbb{P}_0(\sharp\{J_j^\varepsilon\}>n)+\mathbb{P}_0\left(\exists j\in\{1,..,n-1\}\ J_{j+1}^\varepsilon-J_j^\varepsilon\leq\delta,\ \sharp\{J_j^\varepsilon\}\leq n\right)\\ &\leq \eta+\sum_{j=1}^{n-1}\mathbb{P}_0(J_{j+1}^\varepsilon-J_j^\varepsilon\leq\delta)\end{aligned} \tag{S.14}$$

Moreover, for any $j\in\{1,..,n-1\}$,

$$\mathbb{P}_0(J_{j+1}^\varepsilon-J_j^\varepsilon\leq\delta)\leq\mathbb{P}_0(J_{j+1}^\varepsilon-J_j^\varepsilon\leq\delta|X^\varepsilon(J_j^\varepsilon)=0)+\mathbb{P}_0(X^\varepsilon(J_j^\varepsilon)\geq1) \tag{S.15}$$

The first term of the r.h.s of (S.15) can be bounding using the Markov property of $(M^\varepsilon, Z^\varepsilon, C^\varepsilon, X^\varepsilon, D^\varepsilon)$. Indeed, the two last types of events (10 and 11) can not occur after time J_j^ε

and before any other jumps, since $X^\varepsilon(J_j^\varepsilon) = 0$. Hence

$$\mathbb{P}_0(J_{j+1}^\varepsilon - J_j^\varepsilon \le \delta | X^\varepsilon(J_j^\varepsilon) = 0) \le \mathbb{P}_0\left(\exists i \in \{1,..,9\}, \int_0^\delta \int_{\mathbb{R}^+} \mathbf{1}_{\{\theta \le r_i^\varepsilon(s-)\}} N^i(\mathrm{d}s, \mathrm{d}\theta) \ge 1\right)$$
$$\le \delta \sum_{i=1}^{9} \mathbb{E}_0\left[\sup_{s\in[0,T]} r_i^\varepsilon(s)\right] \le \delta C_2 \le \frac{\eta}{n},$$

as soon as $\delta \le \eta/(nC_2)$. Hence, with (S.14) and (S.15),

$$\mathbb{P}_0(\exists j \ge 0, J_{j+1}^\varepsilon - J_j^\varepsilon \le \delta) \ \le \ 2\eta + \sum_{j=1}^{n-1} \mathbb{P}_0(X^\varepsilon(J_j^\varepsilon) \ge 1). \tag{S.16}$$

To bound the second term of the r.h.s of (S.16), recall that the positive jumps of X^ε are not jumps of $\mathbb{Y}^\varepsilon$ and note that $X^\varepsilon(J_j^\varepsilon)$ may be greater than 1 only if there exists a positive jump of X^ε whose next event is of type 1 to 9 (and not of type 10 or 11). We denote the set of positive jumps of X^ε by

$$\{S_\ell^\varepsilon\}_{\ell\ge1} = \{t \in [0,T], X^\varepsilon(t) - X^\varepsilon(t-) = 1\}.$$

The second term of the r.h.s of (S.16) can thus be bounded by

$$\sum_{j=1}^{n-1} \mathbb{P}_0(X^\varepsilon(J_j^\varepsilon) \ge 1) \le \mathbb{P}_0\left(\exists \ell \ge 1, \min_{1\le i\le 9} \tau_i^\varepsilon(S_\ell^\varepsilon) \le \min\{\tau_{10}^\varepsilon(S_\ell^\varepsilon), \tau_{11}^\varepsilon(S_\ell^\varepsilon)\}\right), \tag{S.17}$$

where for any $i = 1,..,10$, $\tau_i^\varepsilon(S_\ell^\varepsilon)$ is the first time event of type i after S_ℓ^ε, that is

$$\tau_i^\varepsilon(S_\ell^\varepsilon) := \inf\left\{t \ge S_\ell^\varepsilon, \int_{S_\ell^\varepsilon}^t \int_{\mathbb{R}^+} \mathbf{1}_{\{\theta \le r_i^\varepsilon(s-)\}} N^i(\mathrm{d}s, \mathrm{d}\theta) \ge 1\right\}.$$

After time S_ℓ^ε and before any other event, X^ε is obviously greater than 1. The rates r_{10}^ε and r_{11}^ε can thus be bounded from below by $\bar\lambda_{-1}^\varepsilon$ and $\bar\mu^\varepsilon$ respectively, other rates can be bounded from above using the r.v. $N_{\max}^\varepsilon$. Thus, using again (S.13), together with (S.17) and the Markov property satisfied by $(M^\varepsilon, Z^\varepsilon, C^\varepsilon, X^\varepsilon, D^\varepsilon)$, we obtain

$$\sum_{j=1}^{n-1} \mathbb{P}_0(X^\varepsilon(J_j^\varepsilon) \ge 1) \le \sum_{\ell=1}^{n} \mathbb{P}_0\left(\min_{1\le i\le 9} \tau_i^\varepsilon(S_\ell^\varepsilon) \le \min\{\tau_{10}^\varepsilon(S_\ell^\varepsilon), \tau_{11}^\varepsilon(S_\ell^\varepsilon)\}\right) + \mathbb{P}_0(\sharp\{S_\ell^\varepsilon\} > n)$$
$$\le n\mathbb{P}_0\left(\tau \le \mathcal{E}_{\bar\lambda_{-1}^\varepsilon + \bar\mu^\varepsilon}\right) + \eta,$$

where $\mathcal{E}_{\bar\lambda_{-1}^\varepsilon+\bar\mu^\varepsilon}$ is an exponential r.v. with parameter $\bar\lambda_{-1}^\varepsilon + \bar\mu^\varepsilon$, and,

$$\tau = \inf\left\{t \ge 0, \int_0^t \int_{\mathbb{R}^+} \mathbf{1}_{\{\theta \le \bar I_C + \bar I_D + C_1 N_{\max}^\varepsilon + \bar\lambda (N_{\max}^\varepsilon)^2\}} N^1(\mathrm{d}s, \mathrm{d}\theta) \ge 1\right\}.$$

Hence

$$\sum_{j=1}^{n-1} \mathbb{P}_0(X^\varepsilon(J_j^\varepsilon) \ge 1) \le n\int_0^\infty \mathbb{P}_0(\tau \le s)(\bar\lambda_{-1}^\varepsilon + \bar\mu^\varepsilon) e^{-(\bar\lambda_{-1}^\varepsilon + \bar\mu^\varepsilon)s} \mathrm{d}s + \eta$$
$$\le n\varepsilon \frac{C_2}{\bar\lambda_{-1} + \bar\mu} + \eta. \tag{S.18}$$

Finally, with (S.11), (S.16) and (S.18), we obtain

$$\limsup_{\varepsilon\to 0}\mathbb{P}(\exists j\geq 0, J^{\varepsilon}_{j+1}-J^{\varepsilon}_{j}\leq\delta)\ \leq\ 4\eta,$$

as soon as $\delta\leq\eta^2/(18TC_2^2)$ (as this implies that $\delta\leq\eta/(nC_2)$). This ends the proof of ii), and the one of the tightness of process $\mathbb{Y}^{\varepsilon}$.

Step 2: The second step is to identify the limit. As the sequence of processes $(\mathbb{Y}^{\varepsilon})_{\varepsilon>0}$ is tight, it is sufficient to prove that any accumulation point has the same law. Let us take $(M,Z,C,D)\in\mathbb{D}([0,T],\mathbb{N}^4)$ the limit (in law) of a sub-sequence of $(\mathbb{Y}^{\varepsilon})_{\varepsilon>0}$, that we denote also by $(\mathbb{Y}^{\varepsilon})_{\varepsilon>0}$ for the sake of readability and we will denote (M,Z,C,D) by $\mathbb{Y}$. We first prove that $\mathbb{Y}$ is a Markov process and then characterize it by describing its jump rates. Note that $\{\mathbb{Y}^{\varepsilon}\}_{\varepsilon>0}$ are not Markov processes, however $\{(\mathbb{Y}^{\varepsilon},X^{\varepsilon})\}_{\varepsilon>0}$ are Markov processes.

To prove that $\mathbb{Y}$ is a Markov process, let us set $t>0$, a sequence of $m+m'$ times $0\leq t_1\leq ...\leq t_m\leq t\leq s_1\leq ..\leq s_{m'}$ and $m+m'+1$ vectors, $y_1,..,y_m,y_t,y'_1,..,y'_{m'}\in\mathbb{N}^4$. From Dynkin's theorem, it is sufficient to prove that

$$\begin{aligned}\mathbb{P}\Big(\mathbb{Y}(s_{m'})=y'_{m'},..,\mathbb{Y}(s_1)=y'_1|\mathbb{Y}(t)=y_t,\mathbb{Y}(t_m)=y_m,..,\mathbb{Y}(t_1)=y_1\Big)\\ =\mathbb{P}\Big(\mathbb{Y}(s_{m'})=y'_{m'},..,\mathbb{Y}(s_1)=y'_1|\mathbb{Y}(t)=y_t\Big).\end{aligned}\tag{S.19}$$

From the convergence in law and assumptions on $X^{\varepsilon}(0)$, we have, for any $\varepsilon>0$,

$$\begin{aligned}&\mathbb{P}\Big(\mathbb{Y}(s_{m'})=y'_{m'},..,\mathbb{Y}(s_1)=y'_1|\mathbb{Y}(t)=y_t,..,\mathbb{Y}(t_1)=y_1\Big)\\ &\qquad=\lim_{\varepsilon\to 0}\mathbb{P}_0\Big(\mathbb{Y}^{\varepsilon}(s_{m'})=y'_{m'},..,\mathbb{Y}^{\varepsilon}(s_1)=y'_1|\mathbb{Y}^{\varepsilon}(t)=y_t,..,\mathbb{Y}^{\varepsilon}(t_1)=y_1\Big)\\ &\qquad=\lim_{\varepsilon\to 0}\frac{\sum_{k\geq 0}\mathbb{P}_0\Big(\mathbb{Y}^{\varepsilon}(s_{m'})=y'_{m'},..,(\mathbb{Y}^{\varepsilon},X^{\varepsilon})(t)=(y_t,k),..,\mathbb{Y}^{\varepsilon}(t_1)=y_1\Big)}{\sum_{k\geq 0}\mathbb{P}_0\Big((\mathbb{Y}^{\varepsilon},X^{\varepsilon})(t)=(y_t,k),..,\mathbb{Y}^{\varepsilon}(t_1)=y_1\Big)}.\end{aligned}\tag{S.20}$$

Then we prove that, for ε small enough, $X^{\varepsilon}(t)$ is equal to 0 with a large probability. Indeed, $(X^{\varepsilon}(u))_{u\leq t}$ has little chance to reach 2:

$$\mathbb{P}_0(\sup_{u\leq t}X^{\varepsilon}(u)\geq 2)\leq\mathbb{P}_0\left(\exists\ell\geq 1,\min_{1\leq i\leq 9}\tau^{\varepsilon}_i(S^{\varepsilon}_{\ell})\leq\min\{\tau^{\varepsilon}_{10}(S^{\varepsilon}_{\ell}),\tau^{\varepsilon}_{11}(S^{\varepsilon}_{\ell})\}\right),$$

where all terms have been defined in (S.17), and the r.h.s term has been proved to converge to 0 when ε goes to 0. It remains to prove that $X^{\varepsilon}(t)$ has little chance to be equal to 1 on $\{\sup_{u\leq t}X^{\varepsilon}(u)\leq 1\}$

$$\mathbb{P}_0\Big(X^{\varepsilon}(t)=1,\ \sup_{u\leq t}X^{\varepsilon}(u)\leq 1\Big)\leq\mathbb{P}_0\Big(\exists\ell\geq 1,\ S^{\varepsilon}_{\ell}\leq t<S^{\varepsilon}_{\ell}+\min\{\tau^{\varepsilon}_{10}(S^{\varepsilon}_{\ell}),\tau^{\varepsilon}_{11}(S^{\varepsilon}_{\ell})\},\ \sup_{u\leq t}X^{\varepsilon}(u)\leq 1\Big).$$

As previously, note that there is not an infinite number of events S^{ε}_{ℓ} in $[0,T]$ and that $\{S^{\varepsilon}_{\ell}\}_{\ell>0}$ are directly correlated to the events of type 9. As $\min\{\tau^{\varepsilon}_{10}(S^{\varepsilon}_{\ell}),\tau^{\varepsilon}_{11}(S^{\varepsilon}_{\ell})\}$ is an exponential random

variable $\mathcal{E}_{\bar\lambda^\varepsilon_{-1}+\bar\mu^\varepsilon}$, we deduce,

$$\begin{aligned}
&\mathbb{P}_0(X^\varepsilon(t)=1,\{\sup_{u\le t}X^\varepsilon(u)\le 1\})\\
&\qquad\le \sum_{\ell\ge 1}^{n}\int_0^\infty \mathbb{P}_0\Big(S^\varepsilon_\ell\in]t-h,t]\Big)(\bar\lambda^\varepsilon_{-1}+\bar\mu^\varepsilon)e^{-h(\bar\lambda^\varepsilon_{-1}+\bar\mu^\varepsilon)}dh+\mathbb{P}_0\left(\sharp\{S^\varepsilon_j\}>n\right)\\
&\qquad\le n\int_0^\infty \mathbb{P}_0\Big(\int_{t-h\vee 0}^{t}\int_{\mathbb{R}^+}\mathbf{1}_{\{\theta\le r^\varepsilon_9(s-)\}}N^9(ds,d\theta)\ge 1\Big)(\bar\lambda^\varepsilon_{-1}+\bar\mu^\varepsilon)e^{-h(\bar\lambda^\varepsilon_{-1}+\bar\mu^\varepsilon)}dh+\eta\\
&\qquad\le n\int_0^\infty h\bar\lambda C_0(\bar\lambda^\varepsilon_{-1}+\bar\mu^\varepsilon)e^{-h(\bar\lambda^\varepsilon_{-1}+\bar\mu^\varepsilon)}dh+\eta\\
&\qquad\le \frac{n\bar\lambda C_0}{\bar\lambda^\varepsilon_{-1}+\bar\mu^\varepsilon}+\eta\le 2\eta,
\end{aligned}$$

as soon as ε is sufficiently small. In other words, $\mathbb{P}_0(X^\varepsilon(t)\ge 1)$ converges to 0 with ε. (S.20) becomes

$$\begin{aligned}
&\mathbb{P}\Big(\mathbb{Y}(s_{m'})=y'_{m'},..,\mathbb{Y}(s_1)=y'_1|\mathbb{Y}(t)=y_t,..,\mathbb{Y}(t_1)=y_1\Big)\\
&\qquad=\lim_{\varepsilon\to 0}\frac{\mathbb{P}_0\Big(\mathbb{Y}^\varepsilon(s_{m'})=y'_{m'},..,(\mathbb{Y}^\varepsilon,X^\varepsilon)(t)=(y_t,0),..,\mathbb{Y}^\varepsilon(t_1)=y_1\Big)}{\mathbb{P}_0\Big((\mathbb{Y}^\varepsilon,X^\varepsilon)(t)=(y_t,0),..,\mathbb{Y}^\varepsilon(t_1)=y_1\Big)}\\
&\qquad=\lim_{\varepsilon\to 0}\mathbb{P}_0\Big(\mathbb{Y}^\varepsilon(s_{m'})=y'_{m'},..|(\mathbb{Y}^\varepsilon,X^\varepsilon)(t)=(y_t,0),..,\mathbb{Y}^\varepsilon(t_1)=y_1\Big)\\
&\qquad=\lim_{\varepsilon\to 0}\mathbb{P}_0\Big(\mathbb{Y}^\varepsilon(s_{m'})=y'_{m'},..|(\mathbb{Y}^\varepsilon,X^\varepsilon)(t)=(y_t,0)\Big),
\end{aligned}\tag{S.21}$$

where we used the Markov property of $(\mathbb{Y}^\varepsilon,X^\varepsilon)$. Using same ideas, it is straightforward to prove that $\mathbb{P}\Big(\mathbb{Y}(s_{m'})=y'_{m'},..|\mathbb{Y}(t)=y_t\Big)$ is also equal to the last term of (S.21), hence (S.19) and the Markov property of $\mathbb{Y}$.

It remains to describe the transition rate matrix of $\mathbb{Y}$. To this aim, for any $y,y'\in\mathbb{N}^4$, we study the limits

$$\lim_{t\to 0}\mathbb{P}\Big(\mathbb{Y}(t)=y'|\mathbb{Y}(0)=y\Big).$$

From what we have seen before (notably that the events of type 1 to 8 are not really affected by the presence of the fast species X^ε), it is straightforward that, in the limiting process $\mathbb{Y}$, there exist 8 types of events with rates $(1-\varphi)\bar\gamma_M\bar V_{mU}\frac{D^\varepsilon}{K_{mU}+D}M\mathbf{1}_{\{D\ge\alpha+\alpha'\}}$ (birth of a M), $\bar d_M M$ (death of a M), $\varphi\bar\gamma_Z\bar V_{mU}\frac{D}{K_{mU}+D}M\mathbf{1}_{\{D\ge\gamma+\gamma'\}}$ (production of a Z), $\bar d_Z Z$ (deactivation of a Z), $\bar I_C$ (appearance of a C), $\bar e_C C$ (disappearance of a C), $\bar I_D$ (appearance of a D), $\bar e_D D$ (disappearance of a D). It remains to deal with the three last types of events. However, we have seen that when a event of type 9 occurs, an event of type 10 or 11 occurs immediately after (such that the formed complex disappears or dissociates). In the limit, both events are simultaneous and

$$\begin{aligned}
&\mathbb{P}\Big(\mathbb{Y}(t)=(m_0,z_0,c_0-1,d_0+\beta)|\mathbb{Y}(0)=(m_0,z_0,c_0,d_0)\Big)\\
&=\lim_{\varepsilon\to 0}\mathbb{P}\Big(\mathbb{Y}^\varepsilon(t)=(m_0,z_0,c_0-1,d_0+\beta)|\mathbb{Y}^\varepsilon(0)=(m_0,z_0,c_0,d_0)\Big)\\
&=\lim_{\varepsilon\to 0}\mathbb{P}\Big(\mathbb{Y}^\varepsilon(t)=(m_0,z_0,c_0-1,d_0+\beta)|\mathbb{Y}^\varepsilon(0)=(m_0,z_0,c_0,d_0)\Big)
\end{aligned}$$

It remains to characterize the jumps rate of $\mathbb{Y}$. Let us start with a birth of a M. As done previously (see (S.20)-(S.21)), we have

$$\begin{aligned}\mathbb{P}\Big(\mathbb{Y}(t+h) = (m+1,z,c,d-(\alpha+\alpha'))\Big|\mathbb{Y}(t) = (m,z,c,d)\Big)\\ = \lim_{\varepsilon\to 0}\mathbb{P}_0\Big((\mathbb{Y}^\varepsilon,X^\varepsilon)(t+h) = (m+1,z,c,d,0)\Big|(\mathbb{Y}^\varepsilon,X^\varepsilon)(t) = (m,z,c,d,0)\Big).\end{aligned}$$

Using the jumps rate of $(\mathbb{Y}^\varepsilon,X^\varepsilon)$, we deduce directly

$$\mathbb{P}\Big(\mathbb{Y}(t+h) = (m+1,z,c,d-(\alpha+\alpha'))\Big|\mathbb{Y}(t) = (m,z,c,d)\Big) = (1-\varphi)\bar{\gamma}_M\bar{V}_{mU}\frac{d}{\bar{K}_{mU}+d}m\mathbf{1}_{\{d\geq\alpha+\alpha'\}}h+o(h).$$

The same can be done with the death of a M, the production of a Z, the deactivation of a Z, the (dis)appearance of a C and the (dis)appearance of a D, where the actions of the complexes do not intervene. And we find the rate given by Theorem (1) The only problem may come from the decomposition of a C into β D:

$$\begin{aligned}&\mathbb{P}\Big(\mathbb{Y}(t+h) = (m+1,z,c-1,d+\beta)\Big|\mathbb{Y}(t) = (m,z,c,d)\Big)\\ &\quad= \lim_{\varepsilon\to 0}\mathbb{P}_0\Big((\mathbb{Y}^\varepsilon,X^\varepsilon)(t+h) = (m,z,c-1,d+\beta,0)\Big|(\mathbb{Y}^\varepsilon,X^\varepsilon)(t) = (m,z,c,d,0)\Big)\\ &\quad= \lim_{\varepsilon\to 0}\mathbb{P}_0\Big((\mathbb{Y}^\varepsilon,X^\varepsilon)(h) = (m,z,c-1,d+\beta,0)\Big|(\mathbb{Y}^\varepsilon,X^\varepsilon)(0) = (m,z,c,d,0)\Big)\\ &\quad= \lim_{\varepsilon\to 0}\mathbb{P}_0\Big(S_1^\varepsilon\leq h,\tau_{11}^\varepsilon(S_1^\varepsilon)\leq\min_{1\leq i\leq 10}\tau_i^\varepsilon(S_1^\varepsilon))\Big).\end{aligned}$$

As we proved before that $\mathbb{P}_0\left(\min_{1\leq i\leq 9}\tau_i^\varepsilon(S_1^\varepsilon)\leq\tau_{10}^\varepsilon(S_1^\varepsilon)\right)$ converges to 0 with ε (see (S.18)), we have

$$\begin{aligned}&\mathbb{P}\Big(\mathbb{Y}(t+h) = (m+1,z,c-1,d+\beta)\Big|\mathbb{Y}(t) = (m,z,c,d)\Big)\\ &\quad= \lim_{\varepsilon\to 0}\mathbb{P}_0\Big(S_1^\varepsilon\leq h,\tau_{11}^\varepsilon(S_1^\varepsilon)\leq\tau_{10}^\varepsilon(S_1^\varepsilon))\Big)\\ &\quad= \lim_{\varepsilon\to 0}\left(\bar{\lambda}zc\times\frac{\bar{\mu}^\varepsilon}{\bar{\mu}^\varepsilon+\bar{\lambda}_{-1}^\varepsilon}h+o(h)\right)\\ &\quad= \bar{V}_{mD}zch+o(h).\end{aligned}$$

□

5 Supplementary figures

5.1 Figure S1. Effect of K on the dynamics of the total cell population M.

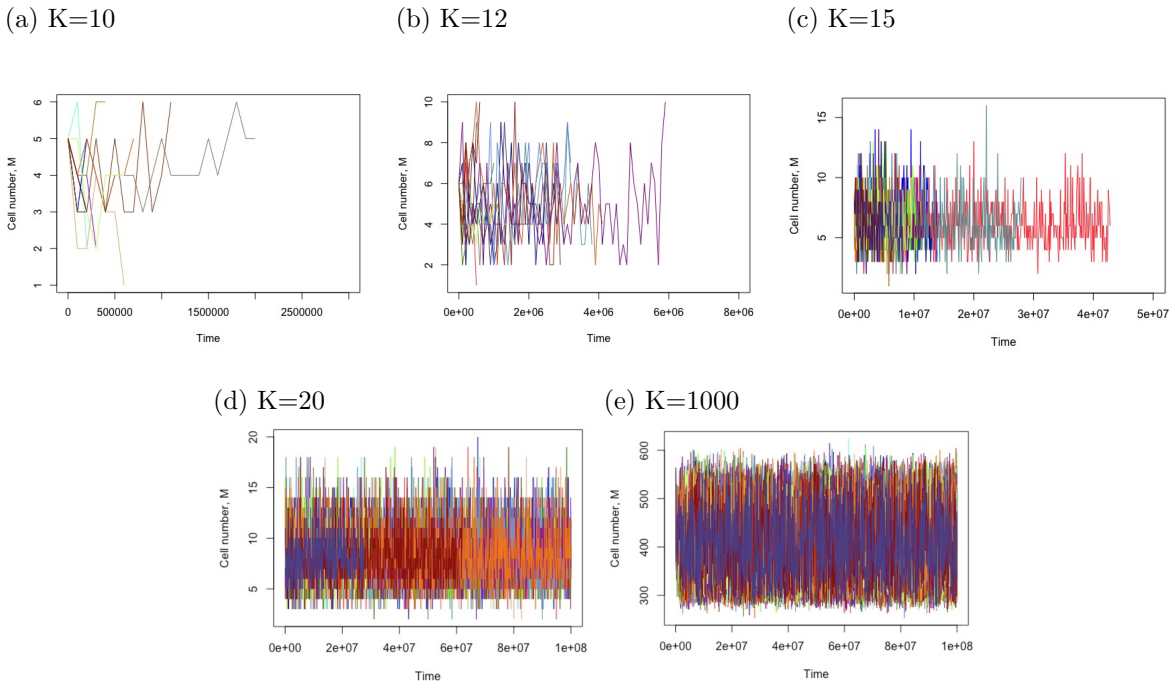

Figure S1. Effect of K on the dynamics of the total cell population M. The model used is the single-microsite hybrid stochastic-deterministic model. Five values of K are used between 10 and 1000. For each value of K, twenty simulation runs are reported; each run is colored differently. Simulations stop when the cell population reaches zero. Parameter values: All constant parameters are set to their default values (Table S3), initial conditions are adjusted to $\varphi = 0.5$, and $T_{\max} = 10^8$.

5.2 Figure S2. Effect of exoenzyme production φ on the dynamics of total cell population M and total mass of z, c, and d.

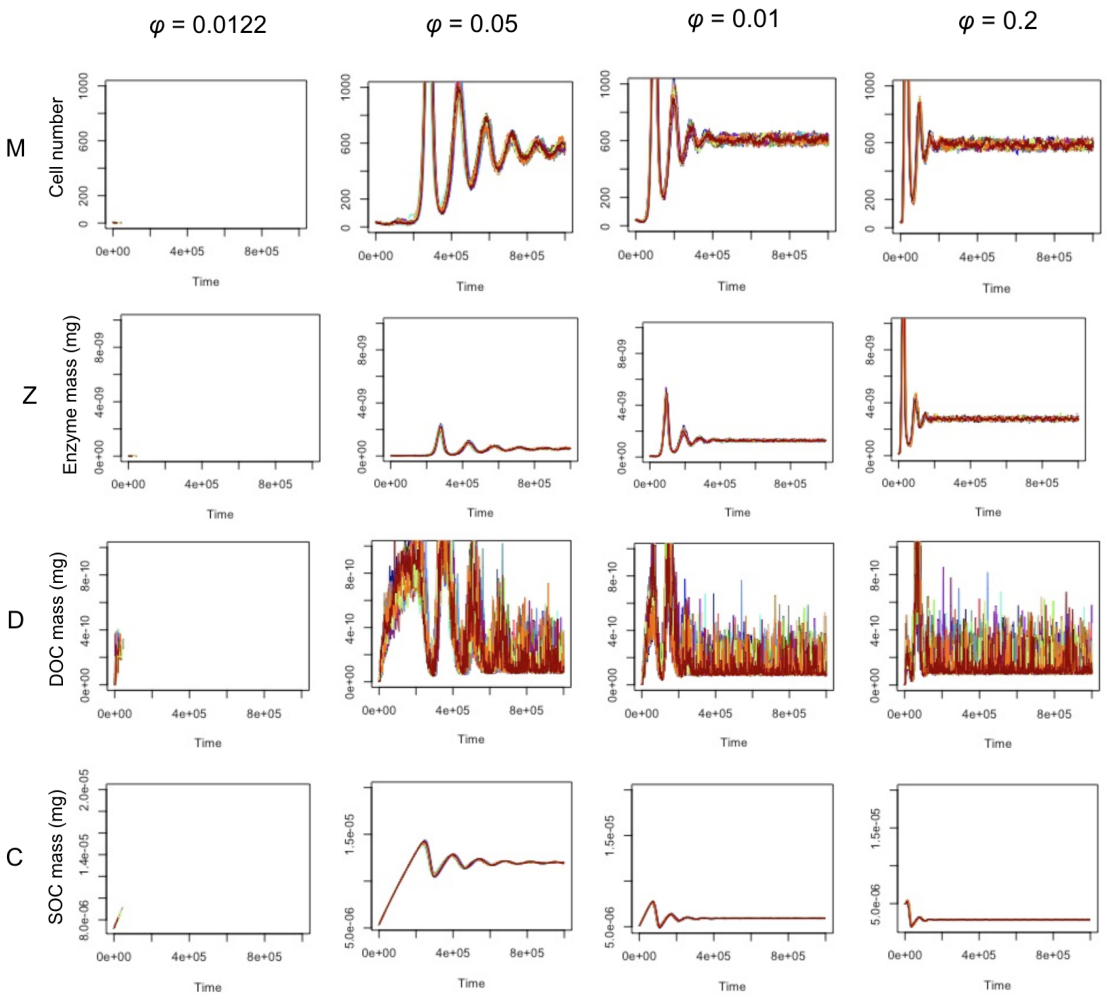

Figure S2. Effect of exoenzyme production φ on the dynamics of total cell population M and total mass of z, c, and d. The model used is a 100-microsites hybrid stochastic-deterministic model with $K = 10$ for all microsites. Parameter values: All constant parameters are set to the default values (Table S3). Initial conditions are set to the steady state of the corresponding φ in the central microsites occupied by microbes, and $M = Z = D = 0$ and $C = 5 \times 10^{-5}$ in the empty microsites.

References

Elsa Abs and Régis Ferrière. Modeling microbial dynamics and soil respiration, effect of climate change. in biogeochemical cycles: Ecological drivers and environmental impact. American Geophysical Union, 2020.

Steven D Allison, Matthew D Wallenstein, and Mark A Bradford. Soil-carbon response to warming dependent on microbial physiology. Nature Geoscience, 3(5):336, 2010.

Patrick Billingsley. Convergence of probability measures. John Wiley & Sons, 2013.

Nicolas Champagnat, Régis Ferrière, and Sylvie Méléard. Unifying evolutionary dynamics: from individual stochastic processes to macroscopic models. Theoretical population biology, 69(3): 297–321, 2006.

Alina Crudu, Arnaud Debussche, Aurélie Muller, Ovidiu Radulescu, et al. Convergence of stochastic gene networks to hybrid piecewise deterministic processes. The Annals of Applied Probability, 22(5):1822–1859, 2012.

Stewart N Ethier and Thomas G Kurtz. Markov processes: characterization and convergence, volume 282. John Wiley & Sons, 2009.

Noah Fierer, Michael S Strickland, Daniel Liptzin, Mark A Bradford, and Cory C Cleveland. Global patterns in belowground communities. Ecology letters, 12(11):1238–1249, 2009.

Nicolas Fournier and Sylvie Méléard. A microscopic probabilistic description of a locally regulated population and macroscopic approximations. The Annals of Applied Probability, 14(4): 1880–1919, 2004.

Stefan AH Geritz, Géza Mesze, Johan AJ Metz, et al. Evolutionarily singular strategies and the adaptive growth and branching of the evolutionary tree. Evolutionary ecology, 12(1):35–57, 1998.

Donovan P German, Kathleen RB Marcelo, Madeleine M Stone, and Steven D Allison. The m ichaelis–m enten kinetics of soil extracellular enzymes in response to temperature: a cross-latitudinal study. Global Change Biology, 18(4):1468–1479, 2012.

Shannon B Hagerty, Kees Jan Van Groenigen, Steven D Allison, Bruce A Hungate, Egbert Schwartz, George W Koch, Randall K Kolka, and Paul Dijkstra. Accelerated microbial turnover but constant growth efficiency with warming in soil. Nature Climate Change, 4(10):903, 2014.

Andrzej M Kierzek. Stocks: Stochastic kinetic simulations of biochemical systems with gillespie algorithm. Bioinformatics, 18(3):470–481, 2002.

Joshua P Schimel and Michael N Weintraub. The implications of exoenzyme activity on microbial carbon and nitrogen limitation in soil: a theoretical model. Soil Biology and Biochemistry, 35(4): 549–563, 2003.

William R Wieder, Steven D Allison, Eric A Davidson, Katerina Georgiou, Oleksandra Hararuk, Yujie He, Francesca Hopkins, Yiqi Luo, Matthew J Smith, Benjamin Sulman, et al. Explicitly representing soil microbial processes in earth system models. Global Biogeochemical Cycles, 29 (10):1782–1800, 2015.